Muxworthy, AR, **Magnetic hysteresis and rotational hysteresis properties of hydrothermally grown multidomain magnetite**, GEOPHYS J INT, 2002, Vol: 149, Pages: 805 - 814, ISSN: 0956-540X

Magnetic hysteresis and rotational hysteresis properties of hydrothermally grown multidomain magnetite

A. R. Muxworthy*

Institut für Allgemeine und Angewandte Geophysik, Universität München, Munich, Germany.

Submitted: 25 May 2001

Summary

A series of hysteresis and rotational hysteresis measurements have been made on a suite of sized hydrothermally-grown multidomain magnetite samples. These measurements consisted of hysteresis measurements between room temperature and the Curie temperature, remanent hysteresis measurements at room temperature, and rotational hysteresis measurements also made at room temperature. It was found that several of the measured and calculated parameters, *e.g.,* the coercive force and rotational hysteresis parameters, display slight grain-size dependencies across the entire range of samples up to the largest sample which has a mean grain size of 108 μm, whereas other results, *e.g.*, Henkel plots, were grain-size independent. These results suggest that there is no clear pseudo-single domain to "true" multidomain behavioural transition. On comparison of high-temperature hysteresis with micromagnetic calculations there appears to be a change in the dominant domain-wall pinning mechanism with temperature. It is suggested that this effect could provide a possible mechanism for domain wall re-organisation models which have been developed to explain partial thermoremanence cooling behaviour. The room temperature rotational hysteresis results indicate that in addition to anisotropy which controls most of the magnetic behaviour, there is a much smaller very high intrinsic anisotropy. It is tentatively suggested that this very high intrinsic anisotropy could be related to metastable remanences in multidomain magnetite. On comparison with published "Crossover" template plots it is seen that the low-dislocation density hydrothermally produced samples display behaviour which does not entirely correspond with the standard templates, implying that the template plots need to be re-assessed.

Key words: rock magnetism, magnetic hysteresis, rotational hysteresis losses, multidomain particles, magnetite.

---

* Now at Dept. of Physics, University of Toronto, 60 St. George St., Toronto, Ontario, M5S 1A7, Canada. Email:

1 Introduction

To understand the behaviour of the natural remanent magnetisation (NRM) of rocks an insight into the magnetic structure of the magnetic minerals and grain sizes which carry this remanence is desired. Multidomain (MD) magnetite is a common carrier of remanence, however, the behaviour and in particular the cause of its high stability is not thoroughly understood. The high stability is thought to be related to areas of stress-controlled metastable domain configurations (McClelland & Shcherbakov, 1995; McClelland *et al.,* 1996; Shcherbakova *et al.,* 1996), however the exact origin of this stress is uncertain. The magnetic behaviour of MD magnetite is investigated further in this paper.

When studying fundamental problems in rock magnetism it is often better to use synthetic samples which are normally more better characterised than natural samples. There are various methods of producing synthetic samples of magnetite, however, no single technique is suitable for producing samples of any given grain-size distribution, spatial distribution, internal stress level *etc.* Therefore, depending on the type of sample required different techniques have to be employed. The synthesis of small single domain (SD) and sub-micron pseudo-single domain (PSD) magnetite with narrow grain-size distributions is relatively straight forward (*e.g.,* Sugimoto & Matijevic 1980), and the magnetic behaviour of SD and PSD grains has been reported in detail by several authors over the last 40 years (*e.g.,* Dunlop & West 1969; Dunlop, 1987; Maher 1988; Schmidbauer & Keller 1996; King & Williams, 2000).

Our knowledge of larger grains, *i.e.,* > 5 μm, is less coherent, as it appears that the method of synthesis strongly effects the magnetic properties of the sample (Hunt *et al.,* 1995). There are primarily three common methods of producing MD magnetite samples of known grain size; crushing or grinding stoichiometric magnetite often of natural origin (*e.g.,* Parry 1965; 1979; Dunlop & Özdemir, 2000), growing synthetic grains in a matrix by the glass-ceramic method (Worm & Markert 1987a), and thirdly by growing crystals using the hydrothermal recrystallisation method (Heider & Bryndzia 1987). Both of the first two methods produce samples which are relatively high in stress, higher than is often found in natural samples (Dunlop & Özdemir, 1997). In contrast the hydrothermal recrystallisation method produces samples with exceptionally low-dislocation

adrian@physics.utoronto.ca

densities, in fact, lower than is found in many but not all natural crystals (Özdemir 2000). In addition to the stress control there are other problems with all three methods of synthesis; the crushing method suffers in that even if the original magnetite is stoichiometric there is evidence to suggest that oxidation occurs during grinding (Day *et al.* 1977), and with both the glass-ceramic and hyrdrothermal recrystallisation methods it is difficult to produce narrow grain-size distributions.

It is possible to anneal samples to reduce the levels of internal stress (*e.g.,* Dankers & Suigiura, 1981, Smith & Merrill, 1984; Dunlop & Xu, 1993), however, this does not reduce stress levels in crushed and glass-ceramic samples to those found in hydrothermally recrystallised samples. For example consider the study of Dankers and Sugiura (1981), they found that the effect of annealing a crushed natural magnetite sample with grain size-range 5-10 μm and concentration of ≈0.1% by weight was to reduce the coercive force which is thought to be an indicator of internal stress, from ≈13 mT to ≈7 mT. In comparison Heider *et al,* (1987) measured coercive force values of 1.1 mT and 0.9 mT for hydrothermally-produced magnetite samples with mean respective grain-sizes of 4.6 μm and 11 μm.

By studying high- and low-stressed samples, the outer limits of magnetic behaviour are in effect being studied. High-stress large MD magnetite samples have been relatively well studied (*e.g.,* Parry 1965; 1979, Day *et al.* 1977, Dankers 1978; Worm & Markert 1987b; Sahu, 1997, Halgedahl 1998, Dunlop & Özdemir, 2000), but low-stress samples have not been studied so extensively. This is partially because the hydrothermal-recrystallisation technique is relatively new to rock magnetism, and secondly because of the time needed to make such samples. Currently, studies from only four separate batches of hydrothermal recrystallised magnetites have been reported in the literature (*i.e.,* Heider *et al*. 1987; 1988; 1992; 1996; Muxworthy 1999; 2000; Muxworthy & McClelland 2000; King & Williams, 2000). The studies of these four batches have covered many different rock magnetic problems and aspects, *e.g.*, low-temperature magnetic properties (Muxworthy 1999; Muxworthy & McClelland 2000; King & Williams 2000), domain observations with temperature (Heider *et al.* 1988), partial-thermoremanence behaviour (Muxworthy 2000), as well as standard characterisation experiments (Heider *et al*.1987). However, there are still a number of standard rock magnetic experiments for which their properties have not been reported

The purpose of this paper is to report for the first time magnetic hysteresis properties of previously-prepared low-stress MD hydrothermally-recrystallized magnetite samples in attempt to advance our

knowledge of MD magnetite's magnetic character. Because of these samples' unique character understanding their behaviour in relation to stressed samples provides crucial information about the effect of stress. In this paper three aspects of hysteresis are reported; hysteresis as a function of high- temperature, remanent hysteresis measured at room-temperature and the rarely analysed rotational hysteresis loss also measured at room temperature. Low-temperature hysteresis behaviour has been previously reported for these same samples (Muxworthy 1999).

By examining hysteresis as a function of temperature it is possible to gain a better understanding of the dominant magnetic mechinisms which control the magnetisation at different temperatures. In particular these results are important to thermoremanence acquisition theories (Néel, 1955). Remanent hysteresis measurements is a common method of identifying the grain-size and mineralogy of sample (*e.g.*, Symons & Cioppia, 2000). However, they also provide information about the coercive spectrum of a sample and they can be used to assess the degree of interactions within a sample (Henkel, 1964).

Rotational hysteresis loss measurements give information about the influence of various kinds of anisotropies on irreversible magnetisation processes. In most conventional magnetic measurements both reversible and irreversible magnetisation processes contribute to the total magnetic signal, however, because in rotational hysteresis loss measurements only the irreversible magnetisation processes contribute, it is possible to examine small irreversible features which cannot normally be observed. Rotational hysteresis loss, W_{RH}, is the energy required to rotate a ferro- or ferrimagnet quasi-statically through 360° in a constant magnetic field (Bozorth 1951; Stacey & Banerjee 1974). Ideally the W_{RH} should be measured continuously, however, it takes a finite time to measure the torque at various angles, giving rise to a quasi-static approach. W_{RH} is determined by measuring the torque, **T**, exerted on a sample during rotation, firstly clockwise then anti-clockwise or *vice versa*. W_{RH} is defined as one-half of the area enclosed by the **T** versus rotation angle α curves (Bozorth 1951),

$$W_{RH} = \tfrac{1}{2}\int \mathbf{T}(\alpha)d\alpha = \tfrac{1}{2}\int \mu_o I_\perp d\alpha \qquad (1)$$

where $I_\perp$ is the magnetization perpendicular to the instant rotation field H and μ_o is the permeability

of free space. All other components of magnetisation I do not contribute and give $\mathbf{T}(\alpha)=0$. When the applied field is small the magnetisation makes only small reversible excursions about its original direction during field rotation. During full rotation, both the forward and reverse curves are reversible making $W_{RH} = 0$. Reversible curves are also obtained for high fields where the magnetisation vector is always parallel to the applied field. For intermediate values irreversible magnetisation processes become significant giving non-zero values for W_{RH}. Detailed theoretical interpretation of rotational hysteresis curves has been made for SD particles with uniaxial anisotropy of the Stoner-Wohlfarth (SW) type (*e.g.,* Jacobs & Luborsky, 1957). While detailed interpretation is currently only possible for SD particles, rotational hysteresis analysis can still provide valuable qualitative information about the irreversible magnetisation processes in MD grains.

In rock magnetism, rotational hysteresis has been used to identify magnetic phases in rocks (*e.g.,* Day *et al.* 1970; Manson 1971), and it has also been used in the detection and study of very high local anisotropies in titanomagnetites (Schmidbauer & Keller 1994; Keller & Schmidbauer 1999b). Previous measurements on magnetite have found evidence for the presence of localised areas of high anisotropy, which is expected to significantly effect thermoremant acquisition. All these studies however were on either ball-milled, very small PSD or stressed samples. By studying hydrothermally crystallised samples for the first time, it is was hoped to discover whether this localised high anisotropy is truly intrinsic to magnetite or whether it is due to stress or non-stoichometry.

2 Sample description and experimental methods

Assemblages of single crystals of MD synthetic magnetite were prepared by hydrothermal recrystallisation (Muxworthy 1998) after the technique described by Heider & Bryndzia (1987). The initial seed material was commercially obtained magnetite (Johnson-Matthey, 99.999 % pure Fe_3O_4, with average diameter $\approx$0.5 μm). Grain size distributions of the samples are summarised in Table 1. The hydrothermal samples had slightly wider grain distributions than the hydrothermal crystals prepared by Heider & Bryndzia (1987). X-ray diffraction (XRD) analysis and Mössbauer spectroscopy were used to determine the chemical composition after hydrothermal recrystallisation, and the samples were found to be stoichiometric magnetite (Muxworthy 1998). For the high-

temperature hysteresis measurements and the remanent hysteresis measurements, the samples were dispersed in KBr pellets in concentrations between 2-3 % by weight. As the samples were only loosely dispersed in KBr the spacing between individual crystals was not accurately controlled.. It is likely therefore, that the magnetite crystals in the samples were subject to magnetostatic grain interactions. However, it has been shown that for magnetite when the grains are much larger than 0.5 μm the importance of particle interaction is relatively small for most in-field magnetic parameters (King, 1996), especially when the samples are dispersed in concentrations < 10 % by weight (Day *et al.*, 1977). Remanence properties appear to be more sensitive to interactions (Day *et al.*, 1977). The KBr pellets were vacuum sealed in quartz capsules to prevent oxidation during heating.

The high-temperature hysteresis measurements were made on two identical variable field translation balances (VFTB) at the Universities of Oxford and Munich. Hysteresis curves were measured for a selection of samples between room temperature and just below the Curie temperature (≈580 °C (Dunlop & Özdemir, 1997)). The maximum applied field was only 230 mT, though this was found to be sufficient to fully saturate all the MD magnetite samples at all temperatures. To check for possible chemical alteration during high-temperature hysteresis measurements, room temperature hysteresis measurements were made after heating. Remanent hysteresis curves were measured using a combination of a pulse magnetiser (maximum field = 800 mT) and CCL cryogenic magnetometer.

Rotational hysteresis measurements were made using an in-house rotational hysteresis magnetometer in Munich. The maximum field used was 1600 mT. For rotational hysteresis it is essential that the particles are fixed during measurement , as unfixed particles are known to give rise to spurious effects (Keller 1997). Fixing particles is best achieved if the particles are set in a highly-viscous fluid which subsequently solidifies. To fix the magnetite crystals were carefully dispersed in heated liquid cetylalcohol (boiling point ≈40 °C). Above 40 °C cetylalcohol is highly viscous making it ideal for fixing the samples for rotational hysteresis experiments. On cooling to room temperature the particles became fixed.

4 Results

4.1 Hysteresis as a function of temperature

Hysteresis curves were measured as a function of temperature for three samples; *H*(7.5 μm), *H*(39 μm) and *H*(76 μm). The hysteresis curves were typical for highly MD materials, and saturated in relatively low fields of around 100 mT. From the hysteresis loops the coercive force, $H_{C,}$ and the ratio of the remanent saturation remanence (M_{RS}) divided by the saturation magnetisation, M_S, were determined and plotted as a function of temperature (Figures 1 and 2). Both H_C and M_{RS}/M_S are seen to decrease with grain size in agreement with other studies for this particular size range (*e.g.,* Day *et al.* 1977*;* Mauritsch *et al.* 1987; Worm & Markert 1987b). The room temperature coercive force values are a little higher than those reported previously for the same samples (Muxworthy & McClelland, 2000). This difference is attributed to the different instruments used to measure the hysteresis curves; in this study the VFTB system was utilized, whereas in the previous study, the hysteresis loops were determined using a Princeton Measurements Alternating Gradient Field Magnetometer (AGFM). Generally H_C is seen to decrease with temperature for all three samples, the rate of decrease rate is almost linear apart from at high temperatures, which suggests that at most temperatures thermofluction effects are not significant in agreement with previous studies on low-stress MD material (Dunlop & Bina, 1977; Heider *et al.,* 1987). Dankers & Sugiura (1981)did not observe such a linear trend in their annealed crushed samples. On approaching the Curie temperature, H_C goes almost to zero, however, it was not possible to measure H_C accurately above 570 °C, due lack of sensitivity in the instrument. The reduced saturation remanence similarly decreases with temperature for all three samples, though this decrease displays less clear trends than the behaviour of H_C (Figures 1 and 2). On approach to the Curie temperature M_{RS}/M_S decreases for the smaller sample, *H*(7.5 μm), but for the larger samples, *i.e., H*(39 μm) and *H*(76 μm), it increases slightly. Whether this is a real effect or not is not clear as on approach to Curie temperature both M_{RS} and M_S tend to zero, increasing measuring errors.

To confirm that no chemical alteration had occurred during measurement at elevated temperatures; repeat room-temperature hysteresis curves were measured. There was found to be no changes in the room-temperature hysteresis parameters.

4.2 Remanent hysteresis curves

Remanent hysteresis curves were measured for all the samples (Figure 3). The remanent hysteresis curves include the isothermal remanence (IRM) acquisition curve from an initially

demagnetised state. For the two curves depicted in Figure 3, it is seen that the IRM acquisition curve and the remanent hysteresis curve do not join until nearly complete remanent magnetisation saturation of the samples, in agreement with previous measurements by Dankers (1981) on crushed natural magnetite samples. From remanent hysteresis curves it is normal to consider both the remanent coercive force (H_{CR}), and remanent acquisition coercive force ($B_{1/2}$), *i.e.,* the field required to reach half remanent saturation on applying a field to an un-magnetised sample (Dankers 1981; Robertson & France 1994). $B_{1/2}$ was calculated from the IRM acquisition curve using the expectation-maximisation algorithm described by Heslop *et al.* (2001). The remanent coercive force was determined by fitting lognormal curves to the first derivative of both the forward and backward acquisition curves. 95 % of the area of both the IRM acquisition curves and the remanent DC demagnetisation curves could be explained by only a single lognormal distribution for all the samples except *H* (39 μm) whose primary component could only explain 89 % of the area. This suggests that magnetic behaviour is primarily controlled by a single consistent pinning mechanism. In Figure 4, $B_{1/2}$ and H_{CR} for the primary component are depicted as a function of grain size. Both parameters display a gradual decrease with grain size. Logarithmic trends have been fitted to the plots, and it is seen that $B_{1/2}$ displays a slightly stronger relationship with grain-size than H_{CR}. Compared to results in the literature the gradients for both $B_{1/2}$ and H_{CR} less than those reported for sized crushed natural magnetites (Dankers 1981), but H_{CR} displays behaviour in agreement with the trends observed by Heider *et al.* (1996) in their review of H_{CR} measurements which included results from hydrothermal recrystallized magnetite samples.

4.3 Rotational hysteresis

Rotational hysteresis loss curves were measured for four samples at room temperature (Figure 5). In Figure 5, only the low-field part of the W_{RH} curves are depicted, though the maximum field applied was 1600 mT. Generally, the curves are quite similar, and display W_{RH} curves typical for MD particles (*e.g.,* Schmidbauer & Keller 1994; Keller & Schmidbauer 1999b). It is useful to quantify the W_{RH} curves using the nomenclature defined in Keller & Schmidbauer (1999b); W_{RHp} is the peak rotational hysteresis loss, W_{1600}/W_{RHp} is ratio of W_{RH} at the maximum field (1600 mT) to W_{RHp}, H_p is the field value for W_{RHp} and $\Delta H_{1/2}$ describes the quantitatively the width of a peak, *i.e.,* it is the full width at half-maximum. These parameters for the four curves in Figure 5 are plotted as a function of grain size in Figure 6.

The maximum height (W_{RHp}) is seen to decrease with grain size in agreement with measurements on sized crushed multidomain titanomagnetite (Keller & Schmidbauer 1999b), however the decrease is nearly linear with grain size, a relationship which has not been reported before for MD grains. The ratio W_{1600}/W_{RHp} is none zero for all four samples. This is contrary to expectations as the hysteresis curves were all closed by a field of ≈200 mT, hence very small irreversible magnetisation processes are giving rise to W_{RH} contributions in Figures 5 and 6 for H > 200 mT. Non-zero W_{1600}/W_{RHp} ratios are reflect a source of high anisotropy within a crystal. Non-zero values of W_{RH} for fields greater than 600 mT have been reported for small-PSD synthetic magnetite particles (Schmidbauer 1988; Schmidbauer & Keller, 1996) and reduced magnetites of natural origin (Dmitriyev *et al.,*1991). In SD grains, high W_{1600}/W_{RHp} ratios usually indicates the presence of an exchange anisotropy between a ferri- or ferromagnetic phase with an antiferromagnetic phase, *e.g.,* between a grain's magnetite core and a surface oxidation layer of hematite (Meiklejohn & Bean 1957). However, as stated previously the rotational hysteresis properties of MD grain are less well understood, and it is thought that surface oxidation products are less important (Schmidbauer & Keller, 1996). The position of the peak values (H_p) is almost identical for the three larger grain sizes, with only *H* (7.5 µm) displaying a lower value (Figure 6c). That the H_p values are fairly consistent for the larger three sizes suggests that the dominant pinning mechanisms throughout the different grain size ranges is the same. That H_p is smaller for *H* (7.5 µm) is surprising as H_p normally decreases with increasing grain size (*e.g.,* Schmidbauer 1988; Keller & Schmidbauer 1999b). The half-width of the curves at full maximum ($\Delta H_{1/2}$) is seen to increase with grain size, suggesting that the width of the distribution of domain wall pinning sites also increases with grain size (Figure 6d). This is consistent with observations on synthetic PSD magnetites (Schmidbauer 1988) and sized titanomagnetite (Keller & Schmidbauer 1999b).

5 Discussion

5.1 Coercive force at high-temperatures

Even though the understanding of hysteresis behaviour of magnetite as a function of temperature is important for rock magnetic MD theories, very few measurements have been reported for well characterised stoichiometric magnetite. Dunlop & Bina (1977) measured hysteresis for a suite of small PSD magnetite samples. Dankers & Sugiura (1981) measured the coercive force on a range of annealed, crushed, sized large MD magnetite samples. Heider *et al.* (1987) have reported the

only measurements on hydrothermally produced magnetites, though this was only for one sample with a mean diameter of 12 μm. Taking the theory of Xu & Merrill (1990), Moskowitz (1993) used a one-dimensional model to examine the effect of various dislocation structures on the normalised coercive force as a function of temperature. The results from this study are compared to the model results in Figure 7. Because the normalised error which becomes quite large especially for sample *H*(75 μm) at high temperatures, error bars are depicted. It should be noted that the model results of Moskowitz (1993) are for a 10 μm grain, implying that the model should only be directly compared to the results for *H*(7.5 μm), which has a similar mean grain size. However, in this study the results for the three different grain sizes display similar behaviour of normalised H_C, suggesting that the pinning mechanisms are relatively independent of grain size. Therefore, it is tentatively suggested that this one-dimensional model can be compared to all three sets of data. Though this interpretation should be treated with caution, as Moskowitz (1993) showed that the microcoercive force due to positive dislocation dipoles displays grain size dependencies. Also depicted in Figure 7 are experimental results of Dunlop & Bina (1977), Dankers & Sugiura (1981) and Heider *et al.* (1987). Only the largest grain size sample of Dunlop & Bina (1977) is shown, which was classified as being in the range 1-5 μm.

Comparing the experimental results of this paper with those of the other three studies, it is seen that normalised H_C displays similar values at lower temperatures to the grown samples Dunlop & Bina (1977) and Heider *et al.* (1987). But this diverges with increasing temperature, and at higher temperatures (> 400 °C) the behaviour of the samples in this study is closer to that of the annealed crushed samples of Dankers & Sugiura (1981). On comparison with the model results of Moskowitz (1993), it is seen that the dominant pinning mechanism appears to change with temperature, *i.e.,* a "combination" model (Moskowitz 1993). At lower-temperatures H_C for all three samples in this study, coincides with line 3, whereas at higher temperatures H_C coincides with lines 1 and 2 (Figure 7), reflecting both a change in pinning dislocation type and possibly reduced defect width size. It is uncertain whether this apparent change in dominant pinning mechanism is real or not. There are two possible sources of error; firstly chemical alteration, however, this option can be discarded as a source of error as room temperature hysteresis parameters were found to be identical to within experimental error on re-measuring after high-temperature heating. The other possibility is lack of sensitivity in the VFTB and/or the relative significance of the VFTB's driving field, though it is seen that the change from type 3 dislocation dominance to type 2 with temperature is out-with the error bars suggesting that this affect is real. Micromagnetic calculations for single crystals of sub-micron

magnetite predict a relatively sharper decrease in H_C at high-temperatures (Muxworthy & Williams 1999).

5.2 Implications for MD thermoremanence acquisition

That the dominant pinning dislocation type appears to change with temperature (Figure 7), could have significant implications for our understanding of thermoremanence acquisition in MD grains which is currently not well understood. The problem lies in our inability to explain the phenomenon found by McClelland & Sugiura (1987), who showed that on cooling partial thermoremanences (pTRM) induced in MD magnetite below their acquisition temperature in zero-field, that the magnetisation does not increase as the spontaneous magnetisation as suggested in the key paper of Néel (1955). This effect is of fundamental importance to the palaeointensity studies as MD remanence is present in most rocks, and if reliable palaeointensities are to be made then it is important to understand MD thermoremanence acquisition. Muxworthy (2000) found similar behaviour for the same samples studied in this paper. That the dominant pinning mechanism changes with temperature is something which is not considered in any theory. This change in dominant pinning sites could provide a mechanism for "domain re-organisation" theories (*e.g.,* McClelland & Sugiura 1987; Shcherbakov *et al.* 1993).

5.3 Further analysis of remanent hysteresis curves

The remanent hysteresis curves, and the parameters derived from them are only weakly dependent on grain size (Figures 3 & 4), suggesting that it is necessary to examine in more detail the shapes of the curves. This is done here, by considering both Crossover plots and Henkel plots.

Symons & Cioppa (2000) recently published "Crossover" templates, which are a combination of IRM acquisition curves and alternating field (AF) demagnetisation of M_{RS} curves. In a previous paper, AF demagnetisation curves for these same hydrothermal samples were reported (Muxworthy & McClelland 2000). The AF demagnetisation curves were measured using an in-house tumbling AF demagnetisation system. Combining the results of this paper with those in the previous paper of Muxworthy & McClelland (2000), three representative Crossover plots are shown in Figure 8. It is seen that the AF demagnetisation curves plot reasonably well on the Crossover plot, that is, the smallest sample plots within the PSD region, and the larger MD samples plot in the MD region,

though there are a slight divergences at higher fields. The IRM acquisition curves do not fit so well onto the templates, as the measured curves rise less steeply than the template curves. The reason for this difference is not clear, however, it should be noted the template curves are constructed from experimental observations on other samples, and as stated previously, the hydrothermal samples in this study are thought to have exceptionally low-dislocation densities; they would be not expected to display "typical" behaviour. It is seen that initially the hydrothermal samples acquire significant remanence at low-fields which may reflect the relatively low-dislocation density. Low-dislocation densities would allow small fields to produce relatively large normalised isothermal remanences. The *H*(7.5μm) sample displays PSD behaviour for the AF demagnetisaiton and MD behaviour for the IRM acquisition curve according to the template plots of Symons & Cioppa (2000), suggesting that the Crossover plot templates need to be re-evaluated. Another subtle feature of interest is the shape of the AF demagnetisation curves for the larger MD samples. The templates suggest that the very largest MD samples should have a concave rather than convex AF demagnetisation curve, but in fact these large MD grains display convex AF demagnetisation curves.

From the remanent hysteresis curves (Figure 3), it is possible to construct so-called Henkel plots (Henkel 1964). This is a plot of remanence lost during DC demagnetisation of an initial M_{RS}, *i.e.,* one half of a remanent hysteresis curve, versus the initial IRM acquisition curve (IRM(acq)), both normalised to M_{RS}, gained for the same field. For SD particles these plots were originally used to analyse the deviation from SW particles (Wohlfarth 1958), which should produce a straight line. In this case, a deviation was normally associated with either interactions or the presence of MD particles. However, it has been pointed out that a straight line may also result from any kind of particle which has identical magnetisation and demagnetisation processes (Gaunt *et al.* 1986). Henkel plots are illustrated for three representative samples in Figure 9. It is seen that all three hydrothermal samples display asymmetrical concave curves and importantly display no clear grain-size dependency, suggesting that the magnetic processes which control the smallest hydrothermal sample *H*(7.5 μm) is almost identical to the magnetic processes operating in the largest sample *H*(108 μm). However, it has to be taken into account that they take place in quite different external field regions. Similar results were found for sized titanomagnetite samples produced by crushing (Keller & Schmidbauer 1999a).

It was suggested by Dankers (1981) that the simple equation $B_{1/2} + H_{1/2} = 2H_{CR}$ holds experimentally, where $H_{1/2}$ is the mean destructive field (MDF), *i.e.,* the field required to AF

demagnetise half the initial M_{RS}. In Muxworthy & McClelland (2000) MDF values for five of the hydrothermal samples examined in this study were reported. Combining the results in this study with those from the previous study, it is possible to test this relationship which was found for crushed natural magnetite samples (Table 2). It is immediately seen that this relationship does not hold. This is not unsurprising, because even though the magnetisation processes during AF demagnetisaton and IRM acquisition are similar, there is no theoretical reason to suggest that this relationship should hold.

5.4 Evidence for high intrinsic anisotropy in PSD magnetite

It is seen that the rotational hysteresis ratio is non-zero for all the samples examined in this study (Figure 5b), indicating the presence of a high-anisotropy. Similar results have been found for synthetic sub-micron magnetites magnetites (Schmidbauer 1988; Schmidbauer & Keller 1996). However, these observations for PSD and MD magnetite are in general disagreement with the behaviour of other PSD and MD material, which typically display zero values for W_{RH} when the applied field is significantly above the field it takes to saturate a sample during hysteresis.

There are four possible causes for this non-zero W_{1600}/W_{RHp} ratio; firstly the samples have an oxidised surface layer of hematite, giving rise to an exchange anisotropy (Meiklejohn & Bean 1957). However, this can be ruled out because, firstly because both Mössbauer spectroscopy and XRD analysis found no evidence for any oxidation products, secondly, the crystals used to make the rotational hysteresis samples had never been heated (apart from during preparation), therefore any surface oxidation products would be expected to be maghemite, not hematite, which would not produce an exchange anisotropy, and thirdly, exchange anisotropy is not thought to be significant for large MD particles (Keller & Schmidbauer 1999b). The second possible cause of the high-anisotropy is high dislocation densities within the crystals which are known to cause non-zero values of the W_{1600}/W_{RHp} in crushed samples (*e.g.,* Keller & Schmidbauer 1999b), but again this hypothesis can be ruled out as hydrothermal samples display other magnetic characteristics which indicate low-dislocation densities (Heider *et al.* 1987). The third possible reason, is the presence of SD-like inclusions within MD crystals, as suggested by Argyle *et al.* (1994). However, SD-like inclusions are unlikely to be the origin of this high anisotropy, as Muxworthy (1998) found no evidence for SD-like inclusions in these samples on examining the unblocking spectrum of induced pTRMs, following the unblocking test procedure described by McClelland *et al.* (1996) and

Shcherbakova *et al.* (1996). The fourth possible cause for non-zero W_{1600}/W_{RHp} ratios is the presence of grain interactions. This is effect is difficult to assess. In-field measurements, *e.g.*, H_C, are generally not effected by interactions in large dispersed MD samples, however, in fact during W_{RHp} measurements only the irreversible component is being examined which is more akin to zero-field remanence measurements. H_{CR} has been found to be more sensitive to interactions than H_C (Day et al., 1977). However, micromagnetic models of interacting PSD grains (Virdee, 1999) suggest that interaction effects should not significant in fields above 300 mT.

There would appear to be no reasonable explanation for this non-zero W_{1600}/W_{RHp} ratio. The fact that it has been observed in all independent studies of magnetite,*e.g.,* Schmidbauer (1988) Schmidbauer and Keller (1996) and Dmitriyev *et al.* (1991), and this study, suggests that this is an intrinsic property of PSD and MD magnetite. Schmidbauer & Keller (1996) attributed this behaviour to the influence of centres of high anisotropy related to a very low fraction of irreversible magnetision processes in an assumed homogenous spinel phase. They suggested that these centres could arise from the action of octahedrally or tetrahedrally coordinated Fe^{2+} ions in the neighbourhood of lattice defects giving rise to a change in the local crystal field. They went on to state that in such a situation it may be possible that the ground state of the Fe^{2+} ions carries an orbital angular momentum, and by spin-orbit coupling a very high magnetocrystalline anisotropy would develop. The action would be similar to an exchange anisotropy. Perhaps these centres are the origin of the metastability of MD magnetite (McClelland & Shcherbakov 1995)**?**

5.5 Implications for the PSD definition

Small grains above the SD/MD threshold size exhibit decreasing stability with increasing grain size, and are termed pseudo-single domain (PSD). As a result, MD grains are usually grouped into PSD grains and “truly” MD grains, *i.e.,* MD grains which display no grain size dependency. The PSD/MD grain-size threshold is ill-defined, because it is dependent on the magnetic property measured, *e.g.,* thermoremanence or hysteresis parameters, and the nature of the samples, *e.g.,* natural, or synthetic crushed (stressed) or hydrothermally grown samples. Initially the PSD/MD threshold was thought to be as low as 5 μm (Stacey 1958), however, this value has increased over the years. H_{CR} measurements on hydrothermal samples suggest a threshold of ≈110 μm (Heider *et al.* 1996), however, the grain-size dependency of M_{RS} has been found to vary continuously up to 3 mm (Dunlop & Özdemir 1997).

Four of the six parameters plotted as a function of grain size in this paper (Figures 4a, 4b, 6a and 6d) display grain size dependencies up to ≈100 μm, but with no evidence of a PSD/MD threshold, albeit it is rather dubious to give estimates for a transition for the diagrams in Figure 6, due to the low-number of data points. On the other hand some parameters display virtually no grain size dependency, *e.g.,* the normalised H_C versus temperature behaviour (Figure 7) and the Henkel plot (Figure 9). It is thought that these size-independent parameters reflect a fairly consistent mode of pinning throughout all the grain sizes and for all temperatures. On combining the results of this paper with that of the literature, it is suggested that either our current models for MD behaviour are incorrect or that there is no such thing as truly MD behaviour for certain magnetic behaviour, instead there are some parameters which are strongly effected by grain size and others not.

6 Conclusions

Several different magnetic hysteresis properties for a set of sized MD low-stress magnetite samples have been reported. Some of the measured parameters, *e.g.,* the coercive force and rotational hysteresis parameters, display slight grain-size dependencies across the entire range of samples up to the largest sample *H* (108 μm). In other cases, *e.g.,* the Henkel plots (Figure 9), no grain size dependency is observed. These observations add the to the general discussion in the literature, and supports the arguments that there is no clear or sharp PSD to "true" MD transition in magnetic behaviour.

Even though the magnetic measurements made were quite different, there are some general conclusions. From all the experiments, the room temperature magnetic properties appear to be dominated by a single consistent pinning mechanism. Though importantly, as is seen from the high-temperature hysteresis measurements, the dominant pinning mechanism or type and size of pinning location is dependent on temperature. This last finding, could be crucial during thermoremanence acquisition, and may go some way to explaining pTRM cooling behaviour by providing a possible mechanism for "domain reorganisation" theories (*e.g.,* McClelland & Sugiura 1987; Shcherbakov *et al.* 1993).

From the measurements of the rotational hysteresis loss of large MD magnetites, there was evidence for a high intrinsic anisotropy. It is tentatively suggested that this high intrinsic anisotropy could be related to the small metastable fraction of MD remanence whose origin is currently not well

understood (*e.g.,* McClelland & Shcherbakov 1995; McClelland *et al.* 1996).

On comparison with the general template Crossover plots of Symons & Cioppa (2000), the data from the hydrothermal MD magnetite samples fits moderately successfully, however, there are still discrepancies which suggest that these template Crossover plots have to be re-evaluated especially the IRM acquisition curves, where the measured curves in this study are seen to rise less sharply than on the template plots (Figure 8). This difference is attributed to the low-dislocation density of the MD samples considered in this study.

Acknowledgements

I would like to thank E. McClelland, E. Schmidbauer and R. Keller for their insightful comments and fruitful discussions, and I would also like to thank W. Williams and an anonymous reviewer for the comments with regard to the paper. In addition I thank B. Moskowitz for providing the raw-data for the theoretical curves in Figure 7, and M. Cioppa for providing the template curves in Figure 8. The preparation of samples and some of the magnetic measurements, were conducted during the tenureship of NERC PhD studentship held at the University of Oxford, England. The remainder of the work was undertaken in Munich and was funded by the European Network for Mineral Magnetic Studies of Environmental Problems (contract number ERBFMRXCT-98-0247).

References

Argyle, K. S., Dunlop, D. J. & Xu, S., 1994. Single domain behaviour of multidomain magnetite grains (abstract), *EOS, Trans. AGU*, **75**, 196.

Bozorth, R. M., 1951. *Ferromagnetism*, Van Nostrand, Toronto.

Dankers, P., 1978. Magnetic properties of dispersed natural iron-oxides of known grain size, *Ph.D. thesis*, University of Utrecht.

Dankers, P., 1981. Relationship between median destructive field and remanent coercive forces for dispersed natural magnetite, titanomagnetite and hematite, *Geophys. J. R. Astron. Soc.*, **64**, 447-461.

Dankers, P. & Sugiura, N., 1981. The effects of annealing and concentration on the hysteresis properties of magnetite around the PSD-MD transition, *Earth Planet. Sci. Lett.*, **56**, 422-428.

Day, R., O'Reilly, W. & Banerjee, S. K., 1970. Rotational hysteresis study of oxidized basalts, *J. Geophys. Res.*, **75**, 375-386.

Day, R., Fuller, M. & Schmidt, V. A., 1977. Hysteresis properties of titanomagnetites: grain size and compositional dependence, *Phys. Earth Planet. Inter.*, **13**, 260-267.

Dunlop, D.J., 1987. Temperature dependence of hysteresis in 0.04–0.22 μm magnetites and implications for domain structure, *Phys. Earth Planet. Inters.*, **46**, 100–119.

Dunlop, D. J. & Bina, M.-M., 1977. The coercive force spectrum of magnetite at high temperatures: evidence for thermal activation below the blocking temperature, *Geophys J. Royal Astron. Soc.*, **51**, 121-147.

Dunlop D. J. & Özdemir, Ö., 1997. *Rock magnetism: Fundamentals and Frontiers*, Cambridge University Press, New York.

Dunlop, D. J., & Özdemir, Ö., 2000. Effect of grain size and domain state on thermal demagnetization tails, *Geophys. Res. Lett.*, **27**, 1311-1314.

Dunlop, D. J. & West, G. F., 1969. An experimental evaluation of single domain theories, *Rev. Geophys.*, **7**, 709-757.

Dunlop, D. J., & Xu, S., 1994. A comparison of methods of granularity and domain structure determination (abstract). *EOS, Trans. A.G.U.,* **74**, 203.

Dmitriyev, S. V., Metallova, V. V. & Petrov, I. N., 1991. Exchange anisotropy in FeO_3O_4-αFe_2O_3 system and high-temperature magnetic memory of magnetite-bearing rocks, *Izv. Earth Phys.,* **27**, 236-240.

Gaunt, G., Hadjipanayis, G. & Ng, D., 1986. Remanence relationships and domain wall pinning in ferromagnets, *J. Magn. Magn. Mater.*, **54-57**, 841-842.

Halgedahl, S. L., 1998. Revisiting the Lowrie-Fuller test: alternating field demagnetization characteristics of single-domain through multidomain glass-ceramic magnetite, *Earth Planet. Sci. Lett.*, **160**, 257-271.

Heider, F. & Bryndzia, L. T., 1987. Hydrothermal growth of magnetite crystals (1µm to 1mm), *Journal of Crystal Growth*, **84**, 50-56.

Heider, F., Dunlop, D. J. & Sugiura, 1987, Magnetic properties of hydrothermally recrystallized magnetite crystals, *Science*, **236**, 1287-1290.

Heider, F., Halgedahl, S. L. & Dunlop, D.J., 1988. Temperature dependence of magnetic domains in magnetite crystals, *Geophys. Res. Lett.*, **15**, 499-502.

Heider, F., Dunlop, D. J. & Soffel, H. C., 1992. Low temperature and alternating field demagnetisation of saturation remanence and thermoremanence in magnetite grains (0.037 µm to 5 mm), *J. Geophys. Res.*, **97**, 9371-9381.

Heider, F., Zitzelsberger, A. & Fabian, K., 1996. Magnetic-susceptibility and remanent coercive force in grown magnetite crystals from 0.1 µm to 6mm, *Phys. Earth Planet. Inter.*, **93**, 239-256.

Henkel, O. 1964. Remanenzverhalten und Wechselwirkung in hartmagnetischen Teilchenkollektiven, *Phys. Stat. Sol.*, **7**, 919-924.

Heslop, D., Dekkers, M. J., Kruiver, P. P. & van Oorschot, I. H. M., 2001. Analysis of isothermal remanent magnetisation acquisition curves using the expectation-maximisation algorithm, *Earth Planet. Sci. Lett.*, **submitted.**

Hunt, C.P., Moskowitz, B.M. & Banerjee, S. K., 1995. Magnetic properties of rocks and minerals, *in A Handbook of Physical Constants, vol. 3*, pp 189–204, ed. T.J. Ahrens, American Geophysical Union, Washington, DC.

Jacobs, L. S. & Luborsky, F. E., 1957. Magnetic anisotropy and rotational hysteresis in elongated fine-particle magnets, *J. Appl. Phys.*, **28**, 467-473.

Keller, R., 1997. Magnetische Eigenschaften und Rotationhysterese von Titanomagnetitpartikeln $Fe_{3-x}Ti_xO_4$ der Zusammensetzung x = 0.6 und x= 0.7 in der Größe von Einbereichs-, Pseudoeinbereichs- und Vielbereichsteilchen, *Ph.D. Thesis,* University of Munich.

Keller, R. & Schmidbauer, E., 1999a. Magnetic hysteresis properties and rotational hysteresis losses of synthetic stress-controlled titanomagnetite ($Fe_{2.4}Ti_{0.6}O_4$) particles-I. Magnetic hysteresis properties, *Geophys. J. Inter.*, **138**, 319-333.

Keller, R. & Schmidbauer, E., 1999b. Magnetic hysteresis properties and rotational hysteresis losses of synthetic stress-controlled titanomagnetite ($Fe_{2.4}Ti_{0.6}O_4$) particles-II. Rotational hysteresis losses,

Geophys. J. Inter., **138**, 334-342.

King, J. G., 1996. Magnetic properties of arrays of magnetite particles produced by electron beam lithography (EBL)*, Ph.D. Thesis*, University of Edinburgh.

King, J. G. & Williams, W., 2000. Low-temperature magnetic properties of magnetite, *J. Geophys. Res.,* **105***,* 16427-16436.

Maher, B. A., 1988. Magnetic properties of some synthetic submicron magnetites, *Geophys. J.*, **94**, 83-96.

Manson, A. J., 1971. Rotational hysteresis measurements on oxidized synthetic and natural titanomagnetites, *Z. Geophys.*, **37**, 431-442.

Mauritsch, H., Becke, M., Kropácek, V., Zelinka, T. & Hejda, P., 1987. Comparison of the hysteresis characteristics of synthetic samples with different magnetite and haematite contents, *Phys. Earth Planet. Inters.*, **46**, 93–99.

McClelland, E. & Sugiura, N., 1987. A kinematic model of TRM acquisition in multidomain magnetite, *Phys. Earth Planet. Int.*, **46**, 9-23.

McClelland, E., & Shcherbakov, V. P., 1995. Metastability of domain state in MD magnetite; consequences for remanence acquisition, *J. Geophys. Res.*, **100**, 3841-3857.

McClelland, E., Muxworthy, A. R. & Thomas, R. M., 1996. Magnetic properties of the stable fraction of remanence in large multidomain (MD) magnetite grains: single-domain or MD?, *Geophys. Res. Lett.*, **23**, 2831-2834.

Meiklejohn, W. H. & Bean, C. P., 1957. New magnetic anisotropy. *Phys. Rev.*, **105**, 904-913.

Moskowitz, B. M., 1993. Micromagnetic study of the influence of crystal defects on coercivity in magnetite. *J. Geophys. Res.*, **98**, 18011-18026.

Muxworthy, A. R., 1998. Stability of remanence in multidomain magnetite, *D.Phil. Thesis*, University of Oxford.

Muxworthy, A. R., 1999. Low-temperature susceptibility and hysteresis of magnetite, *Earth Planet Science Let.*, **169**, 51-58.

Muxworthy, A. R., 2000, Cooling behaviour of partial thermoremanences induced in multidomain magnetite, *Earth Planet. Sci. Lett.*, **184**, 149-159.

Muxworthy, A. R. & McClelland, E., 2000. The causes of low-temperature demagnetization of remanence in multidomain magnetite, *Geophys. J. Inter.*, **140**, 132-146.

Muxworthy, A. R. & Williams, W., 1999. Micromagnetic calculation of coercive force as a function of temperature in pseudo-single domain magnetite, *Geophys. Res. Let.*, **26**, 1065-1068.

Néel, L., 1955. Some theoretical aspects of rock magnetism, *Adv. Phys.*, 191-242.

Özdemir, Ö., 2000. Coercive force of single crystals of magnetite at low temperatures, *Geophys. J. Inter.*, **141**, 351-356.

Parry, L. G., 1965. Magnetic properties of dispersed magnetite powders, *Phil. Mag.*, **11**, 303-312.

Parry, L. G., 1979. Magnetization of multidomain particles of magnetite, *Phys. Earth Planet. Inter.*, **19**, 12-30.

Robertson, D. J. & France, D. E., 1994. Discrimination of remanence-carrying minerals in mixtures, using isothermal remanent magnetization acquisition curves, *Phys. Earth Planet. Inter.*, **82**, 223-234.

Sahu, S., 1997. An experimental study on the effects of stress on the magnetic properties of magnetite*, Ph.D. thesis*, University of Minnesota.

Schmidbauer, E., 1988. Magnetic rotational hysteresis study on spherical 85-160 nm Fe_3O_4 particles, *Geophys. Res. Lett.*, **15**, 522-525.

Schmidbauer, E. & Keller, R., 1994. Magnetic properties and rotational hysteresis of a basalt with homogeneous Ti-rich titanomagnetite grains 10-20 μm in diameter, *Geophys. J. Inter.*, **119**, 880-892.

Schmidbauer, E., & Keller, R., 1996. Magnetic properties and rotational hysteresis of Fe_3O_4 and-Fe_2O_3

particles ≈250 nm in diameter, *J. Magn. Magn. Mater*., **152**, 99-108.

Shcherbakov, V. P., McClelland, E. & Shcherbakova, V. V., 1993. A model of multidomain thermoremanent magnetization incorporating temperature-variable domain structure, *J. Geophys. Res.*, **98**, 6201-6216, 1993.

Shcherbakova, V. V., Shcherbakov, V .P., Schmidt, P. W. & Prévot, M., 1996. On the effect of low-temperature demagnetisation on TRM and pTRMs, *Geophys. J. Int.*, **127**, 379B386.

Smith, G. M., & Merrill, R. T., 1984. Annealing and stability of multidomain magnetite, *J, Geophys. Res.,* **89**, 7877-7882.

Stacey, F. D., 1958. Thermoremanent magnetization (TRM) of multidomain grains in igneous rocks, *Phil. Mag.*, **3**, 1391-1401.

Stacey, F. D. & Banerjee, S. K., 1974. *The Physical Principles of Rock Magnetism*, Elsevier, Amsterdam.

Sugimoto, T. & Matijevic, E., 1980. Formation of uniform spherical magnetite particles by crystallisation from ferrous hydroxide gels, *J. Colloid Interface Sci.*, **74**, 227-243.

Symons, D. T. A. & Cioppa, M. T., 2000. Crossover plots: a useful method for plotting SIRM data in palaeomagnetism, *Geophys. Res. Lett.*, **27**, 1779-1782.

Virdee, D., 1999. The influence of magnetostatic interactions on the magnetic properties of magnetite, *Ph.D. Thesis*, University of Edinburgh.

Wohlfarth, E.P., 1958. Relations between different modes of acquisition of the remanent magnetization of ferromagnetic particles, *Journal of Applied Physics*, **29**, 595-596.

Worm, H.-U. & Markert, H., 1987a. The preparation of dispersed titanomagnetite particles by the glass-ceramic method, *Phys. Earth Planet. Inter*, **46**, 263-270.

Worm, H.-U., & Markert, H., 1987b. Magnetic hysteresis properties of fine particle titanomagnetites precipitated in a silicate matrix, *Phys. Earth Planet. Inters.*, **46**, 84–93.

Xu, S. & Merrill, R. T., 1990. Microcoercivity, bulk coercivity and saturation remanence in multi-domain materials, *J. Geophys. Res.*, **95**, 7083-7090.

Table 1. Summary of the grain distributions for the samples in this study, determined from scanning electron microscope photographs. The distributions were assumed to be Gaussian, where SD is the standard deviation.

Sample name	Mean (μm)	SD (μm)	No. Particles measured
H (3.0 μm)	3.0	2.4	718
H (7.5 μm)	7.5	3.0	217
H (13 μm)	13	3	211
H (24 μm)	18	6	193
H (39 μm)	24	5	264
H (39 μm)	39	9	243
H (59 μm)	59	16	274
H (76 μm)	76	25	190
H (108 μm)	108	31	168

Table 2. Test for the phenomenological relationship $B_{1/2} + H_{1/2} \approx 2H_{CR}$ proposed by Dankers (1981). The MDF ($H_{1/2}$) data was taken from Muxworthy & McClelland (2000).

Sample name	$B_{1/2}$ (mT)	$H_{1/2}$ (mT)	$B_{1/2} + H_{1/2}$ (mT)	$2H_{CR}$ (mT)
H (3.0 μm)	28	6	24	53
H (7.5 μm)	35	17	52	37
H (24 μm)	30	11	41	50
H (59 μm)	30	6	36	32
H (76 μm)	24	7	31	40

Figure 1. Coercive force ($\mu_0 H_C$) as a function of temperature for three samples produced by hydrothermal recrystallisation with mean grain sizes shown in the brackets. The error on the

measurement of $\mu_0 H_C$ is ≈ 0.1 mT.

Figure 2. Reduced remanent magnetisation (M_{RS}/M_S) as a function of temperature for three samples produced by hydrothermal recrystallisation with mean grain sizes shown in the brackets.

Figure 3. Typical remanent hysteresis curves and initial isothermal remanent acquisition curves for samples a) *H* (13 μm) and b) *H* (108μm).

Figure 4. Plots of a) remanent acquisition coercive force ($B_{1/2}$) and b) remanent coercive force (H_{CR}) versus diameter for all the hydrothermal samples in Table 1. Simple logarithmic trend lines have been fitted to the data.

Figure 5. Detail of rotational hysteresis loss for four samples. The maximum applied field was 1600 mT.

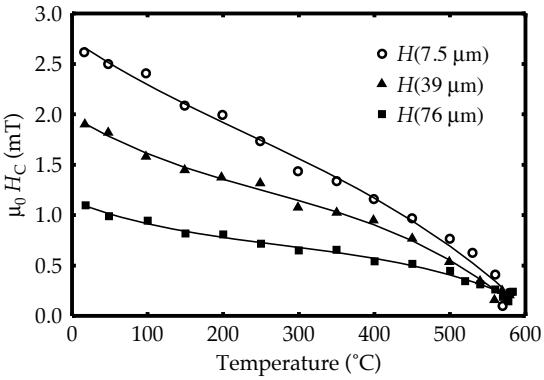
Figure 6. Plots of rotational hysteresis parameters defined in Keller & Schmidbauer (1999) as a function of grain size. a) W_{RHp} is the peak rotational hysteresis loss, b) W_{1600}/W_{RHp} is the ratio of W_{RH} at the maximum field (1600 mT) to W_{RHp}, c) H_p is the field value for W_{RHp} and d) $\Delta H_{1/2}$ describes the quantitatively the width of a peak, *i.e.,* it is the full width at half-maximum. Figure a) has a linear trend line fitted.

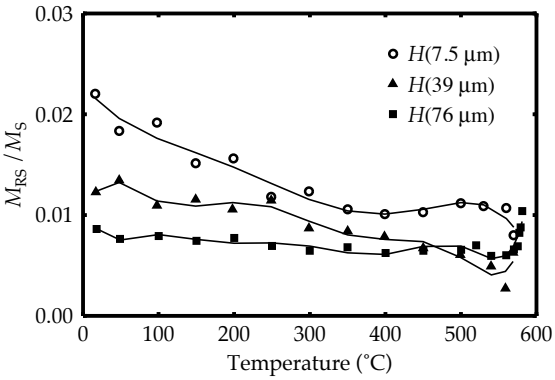
Figure 7. Normalised coercive force versus temperature for the data plotted in Figure 1, with data of Dunlop & Bina (1977), Dankers & Sugiura (1981) and Heider *et al.* (1987) and the theoretical plots of Moskowitz (1993). The samples of Dunlop & Bina (1977) and Heider *et al.* (1987) were both grown synthetic magnetites with mean grain sizes of 1-5 μm and 12 μm respectively. The samples of Heider *et al.* (1987) were made by hydrothermal recrystallisation. The samples of Dankers & Sugiura (1981) were produced by annealing crushed magnetite. The theoretical curves are for a 10 μm grain with(1) positive dislocation dipole, $d/w_0 = 1$, (2) single dislocation, positive dislocation dipole $d/w_0 = 0.1$, or positive dislocation dipole bounding a stacking fault $d/w_0 = 0.1$, (3) negative dislocation dipole, $d/w_0 = 1$, (4) negative dislocation dipole, $d/w_0 = 0.1$, (5) planar defects with exchange pinning $d/w_0 = 0.1$, and (6) for planar defects with anisotropy pinning $d/w_0 = 0.1$, where the ratio d/w_0 is the reduced defect width. This dimensionless parameter sets the size of the defect and remains constant with

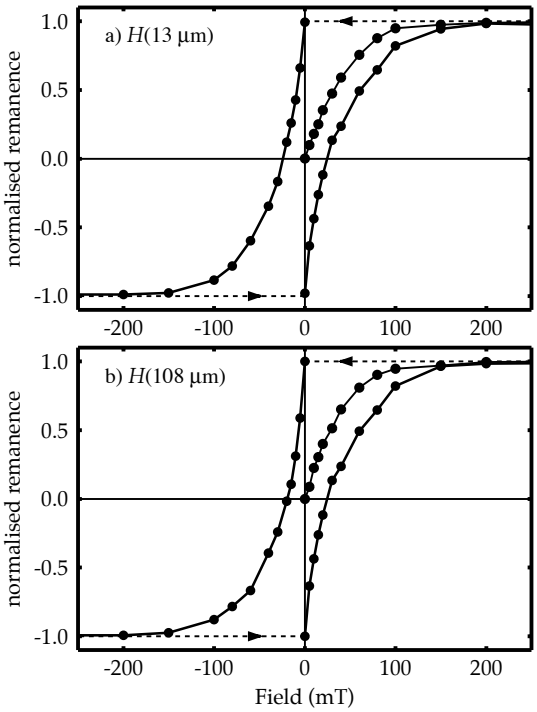
temperature.

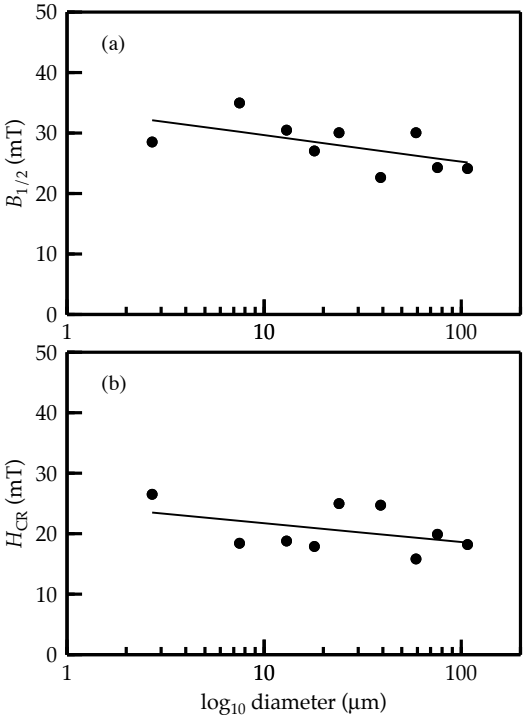
Figure 8. IRM acquisition curves and AF demagnetisation (AF demag) curves for three hydrothermal samples, with the template Crossover plots of Symons & Cioppa (2000). The AF demagnetisation data was taken from Muxworthy & McClelland (2000).

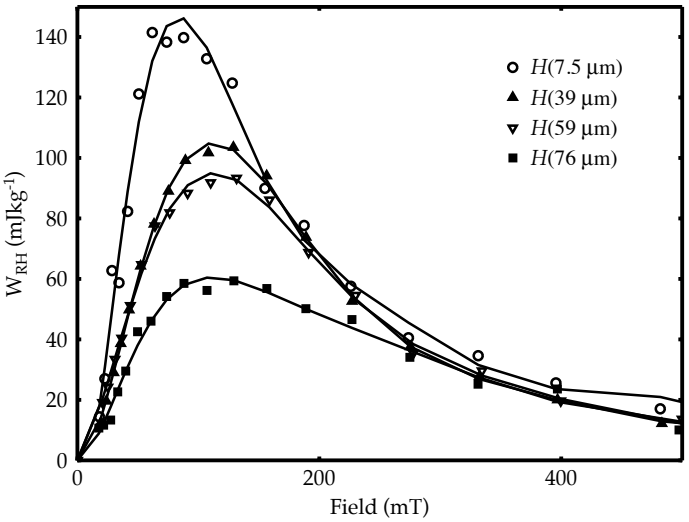
Figure 9. Henkel plots of IRM(acq)/M_{RS} versus IRM(back)/M_{RS} for three representative samples. Three applied field values are labelled for the H(108 μm) sample. The behaviour of an ideal Stoner-Wohlfarth (SW) particle is also depicted.

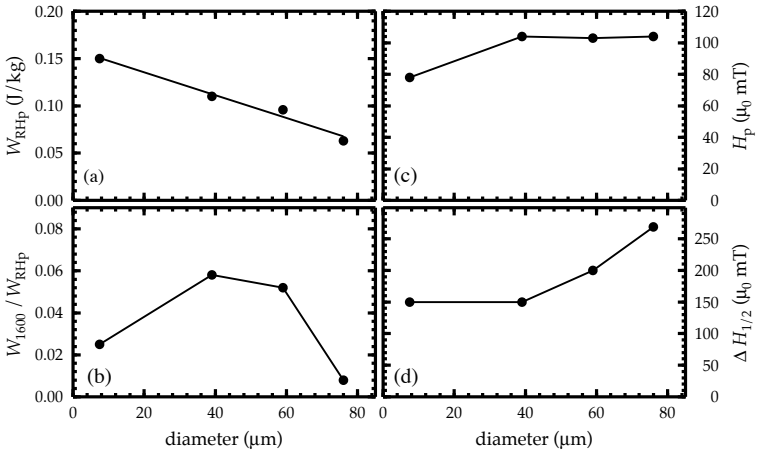

3.0
2.5
2.0
1.5
1.0
0.5
0.0
0
100
200
300
400
500
600
μ0 HC (mT)
Temperature (°C)
H(7.5 μm)
H(39 μm)
H(76 μm)

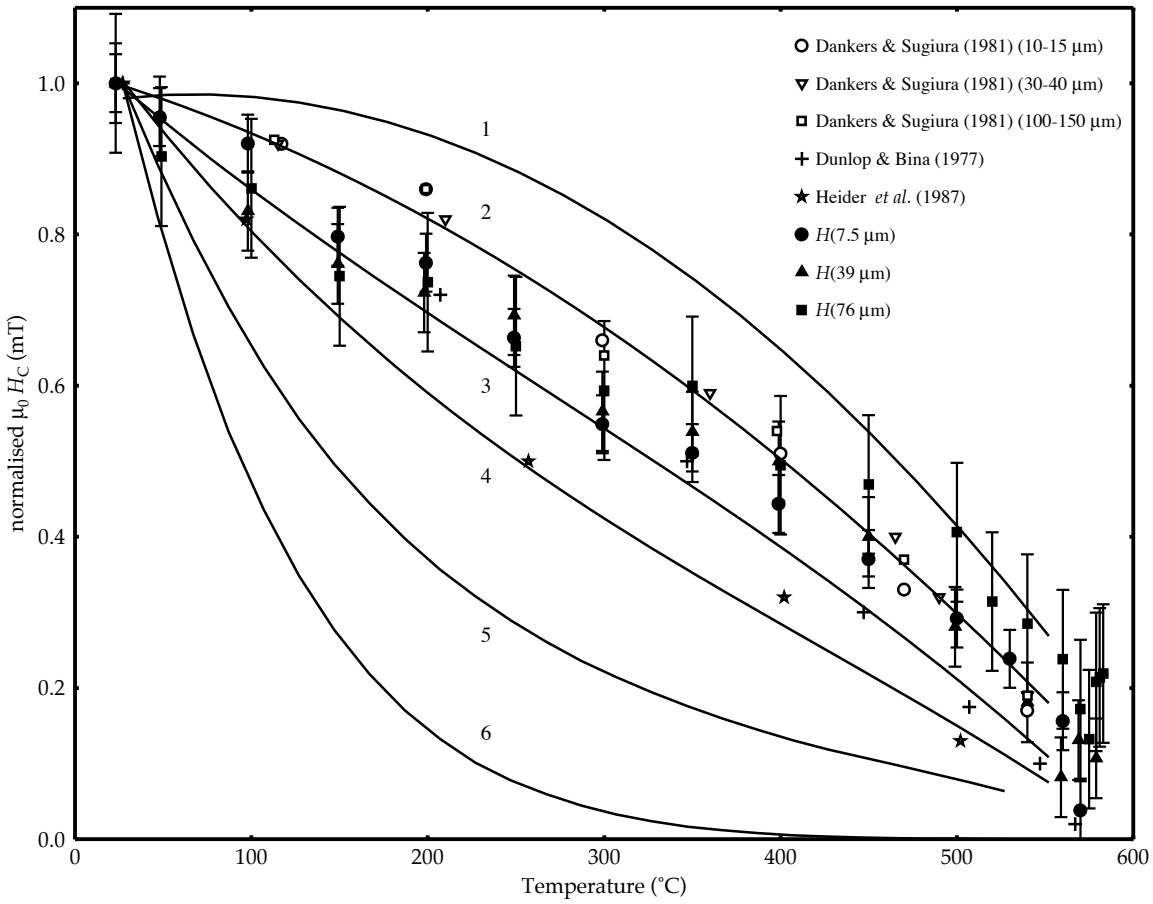

0.03
0.02
0.01
0.00
M_{RS} / M_S
0
100
200
300
400
500
600
Temperature (°C)
H(7.5 μm)
H(39 μm)
H(76 μm)

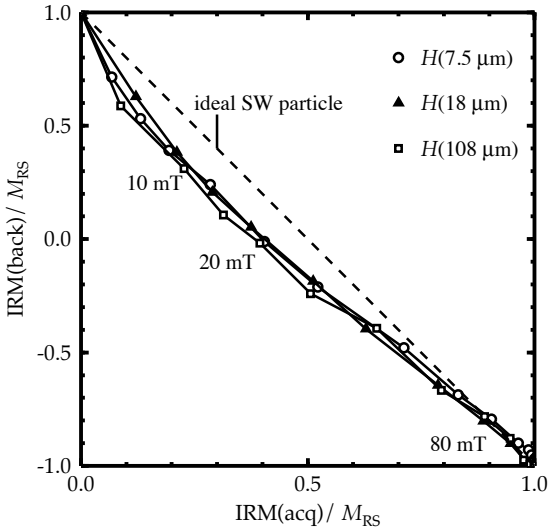

a) H(13 µm)
b) H(108 µm)
normalised remanence
normalised remanence
1.0
0.5
0.0
-0.5
-1.0
-200
-100
0
100
200
Field (mT)


(a)
(b)
$B_{1/2}$ (mT)
H_{CR} (mT)
0
10
20
30
40
50
1
10
100
$\log_{10}$ diameter (μm)


140
120
100
80
60
40
20
0
0
200
400
Field (mT)
W_{RH} (mJkg^{-1})
H(7.5 μm)
H(39 μm)
H(59 μm)
H(76 μm)


0.20
0.15
0.10
0.05
0.00
W_{RHp} (J/kg)
(a)
120
100
80
60
40
20
0
H_p (μ_0 mT)
(c)
0.08
0.06
0.04
0.02
0.00
W_{1600} / W_{RHp}
(b)
250
200
150
100
50
0
$\Delta H_{1/2}$ (μ_0 mT)
(d)
0
20
40
60
80
diameter (μm)
diameter (μm)


Dankers & Sugiura (1981) (10-15 µm)
Dankers & Sugiura (1981) (30-40 µm)
Dankers & Sugiura (1981) (100-150 µm)
Dunlop & Bina (1977)
Heider et al. (1987)
H(7.5 µm)
H(39 µm)
H(76 µm)
1
2
3
4
5
6
normalised µ0 HC (mT)
Temperature (°C)
0.0
0.2
0.4
0.6
0.8
1.0
0
100
200
300
400
500
600


1.0
0.5
0.0
-0.5
-1.0
0.0
0.5
1.0
IRM(back) / M_{RS}
IRM(acq) / M_{RS}
ideal SW particle
H(7.5 μm)
H(18 μm)
H(108 μm)
10 mT
20 mT
80 mT